5.1 Irradiation Response of Next Generation High Temperature Superconducting Rare Earth and Nanoparticle-Doped $YBa_2Cu_3O_{7-x}$ Coated Conductors for Fusion Energy Applications — K. J. Leonard, T. Aytug, Fred. A List III, Yanwen Zhang (Oak Ridge National Laboratory), A. Perez-Bergquist, W.J. Weber (University of Tennessee), and A. Gapud (University of South Alabama)

OBJECTIVE

The goal of this work is to evaluate the irradiation response of the newest generation of coated conductors based on rare earth and nanoparticle doping of the $YBa_2Cu_3O_{7-x}$ (YBCO) high temperature superconductors. The materials under investigation represent different methods for enhanced flux pinning for improved performance under externally applied magnetic fields. Ion beam irradiation will be used to simulate neutron damage cascades in the materials to examine the effect that radiation damage has on the different pre-existing defect structures used for flux pinning and to evaluate the superconductors capability for use in fusion reactor systems.

SUMMARY

During this semiannual reporting period, electrical characterization work was completed on the irradiated superconducting films, and two presentations were made at conferences. The first, "Irradiation Response of Next Generation High Temperature Superconductors for Fusion Energy Applications" was presented at the International Conference of Fusion Reactor Materials in Beijing, China. This presentation introduced the fusion materials community to the advances that have been made in coated conductor technology and the potential for use in nuclear application. The second presentation "Irradiation of Commercial, High-T_c Superconducting Tape for Potential Fusion Application: Electromagnetic Transport Properties," was presented in November at the Southeastern Section American Physical Society Meeting in Bowling Green, KY. This detailed the electrical property characterizations of the conductors and is summarized in this report.

RESULTS

Thin film based coated conductors of Zr-doped $(Y,Gd)Ba_2Cu_3O_{7-x}$ (Zr-YBCO), $(Dy,Y)Ba_2Cu_3O_{7-x}$ (DyBCO) and $Gd_2Ba_2Cu_3O_{7-x}$ (GdBCO) was irradiated by 5 MeV Ni and 25 MeV Au irradiations to fluences between 10^{11} and 10^{12} ions/cm^2. Displacement damage was between 0.003 and 0.03 dpa depending on the type of conductor and its multi-layered architecture as determined through TRIM calculations. Differences in the nominal film thickness of each conductor types accounted for slight variations in dpa of the lower fluence 5 MeV Ni and 25 MeV irradiations and are accounted for in the following text and figures. The difference in dpa between film types for the high fluence 25 MeV Au irradiation was not as significant.

The key issue of interest of these conductors is their ability to pin the flow of magnetic flux quanta, allowing their application in high magnetic fields. In Type II superconductors as the applied magnetic field reaches the first critical field (H_{c1}) quantized vortices begin to penetrate the superconductor. As current is applied the vortices experience Lorentz force, causing vortex flow. The vortex flow is dissipative, effectively killing the superconductivity of the material as the vortices pass through the film even if the applied field is still below the upper critical field (H_{c2}). These latest generations of superconductors are designed to include secondary phase nanoparticles as well as defects that may be correlated to the nanoparticles as sites to trap the vortices. These defects are generally antiphase domain boundaries running in the c-axis

direction (perpendicular to the film) or intergrowths of various chemical compounds based off of variations of the standard Y123 stacking sequence of YBCO running in the *ab* direction.

Figure 1 compares the resistivity as a function of temperature for the three conductors studied following irradiation. The abrupt change from near zero resistivity is the critical temperature (T_c). The transition point identifying the T_c is shown in greater detail within the insert of each plot. The normal state resistivity, the linear portion of the plot at temperatures above the T_c, is increased following irradiation due to the increase in scattering by added defects or impurities. The increase in normal state resistivity increases only a small amount following low fluence irradiation. The irradiation by 5 MeV Ni produces a greater increase in the normal state resistivity over the low fluence 25 MeV Au irradiations in the Zr-YBCO and DyBCO films, though the values of dpa are slightly higher ranging from 0.004 to 0.005 dpa versus 0.003 dpa for the Au irradiations. The GdBCO films show a negative curvature in the normal state resistivity with irradiation, making extrapolation of the residual resistivity (r_i) values at 0 K difficult. For the Zr-YBCO and DyBCO conductors the normal-state is quadratic and identifiable, with the DyBCO conductor having a lower r_i than either the GdBCO or Zr-YBCO materials.

The change in resistivity versus dpa normalized to the pre-irradiated values at 100 K are compared in Figure 2 between the three conductors of this study and that of YBCO deposited on single crystal substrates [1]. The change in resistivity is significantly lower for the conductors of this study compared to the 6 MeV He and 25 MeV O irradiations of Hensel and coworkers. The electronic energy loss value for the 5 MeV Ni is similar to that of the He and O irradiations, while the 25 MeV Au is higher. However, for 120 MeV Kr irradiations the amount of damage created by the swift heavy ions is extensive with large changes in the resistivity measured.

The value of T_c decreases with dpa, though the change is relatively small in the conductors studied suggesting the presence of high-quality superconducting pathways even for the high dose 25 MeV Au irradiations. The dependence of T_c with respect to dpa, shown in Figure 3, further illustrates the reduced sensitivity of these conductors to irradiation. Reduction in T_c is a consequence of displacement reactions changing the whole carrier concentration in the Cu-O chains of the HTS structure, which are the most unstable sites due to the lightly bound oxygen atoms [2]. As oxygen-deficient and highly disordered regions are created with decreasing hole concentrations, degradation in T_c is observed. The relative changes in T_c of all three conductors, before and after the irradiation, is compared to thin YBCO films deposited on single crystal substrates. Note that except for the data of Hensel and coworkers [1] all irradiation studies were conducted near room temperature [3,4]. While increased recombination rates associated with room temperature irradiation may in part contribute to the measured stability, the T_c values of this study are still greater than those of other room temperature irradiated HTS materials. However, the higher irradiation temperatures may not necessarily influence T_c in this manner, as work by Okada and Kawakubo [5] on polycrystalline samples irradiated by neutrons at reactor temperature (360 K) showed a reduction in T_c as compared to irradiation at 20 K. The increased defect mobility at higher irradiation temperatures resulting in subsequent cascade collapse and less flux pinning in the conductor produce larger degradation in critical current density (J_c) [6]. In contrast, the increased defect mobility at higher irradiation temperatures degrades flux pinning and J_c due to the subsequent cascade collapse.

The change in J_c and pinning force (F_p) as a function of applied magnetic field following ion irradiation for the three conductors of this study is presented in Figure 4. The lower fluence ion irradiations have no major detrimental effect on the conductor J_c values, and in the case of DyBCO has an improvement. For the GdBCO conductor, there is a modest effect on J_c at low

fluences, though there is a 30% drop in F_p for irradiations to 0.004 dpa. However, J_c and F_p values for the conductor fall rapidly for the 0.03 dpa irradiation, despite the conductor still being superconducting. This loss is attributed to the disappearance of the Gd_2O_3 nanoparticles in the microstructure and changes in the defects within the conductor following irradiation.

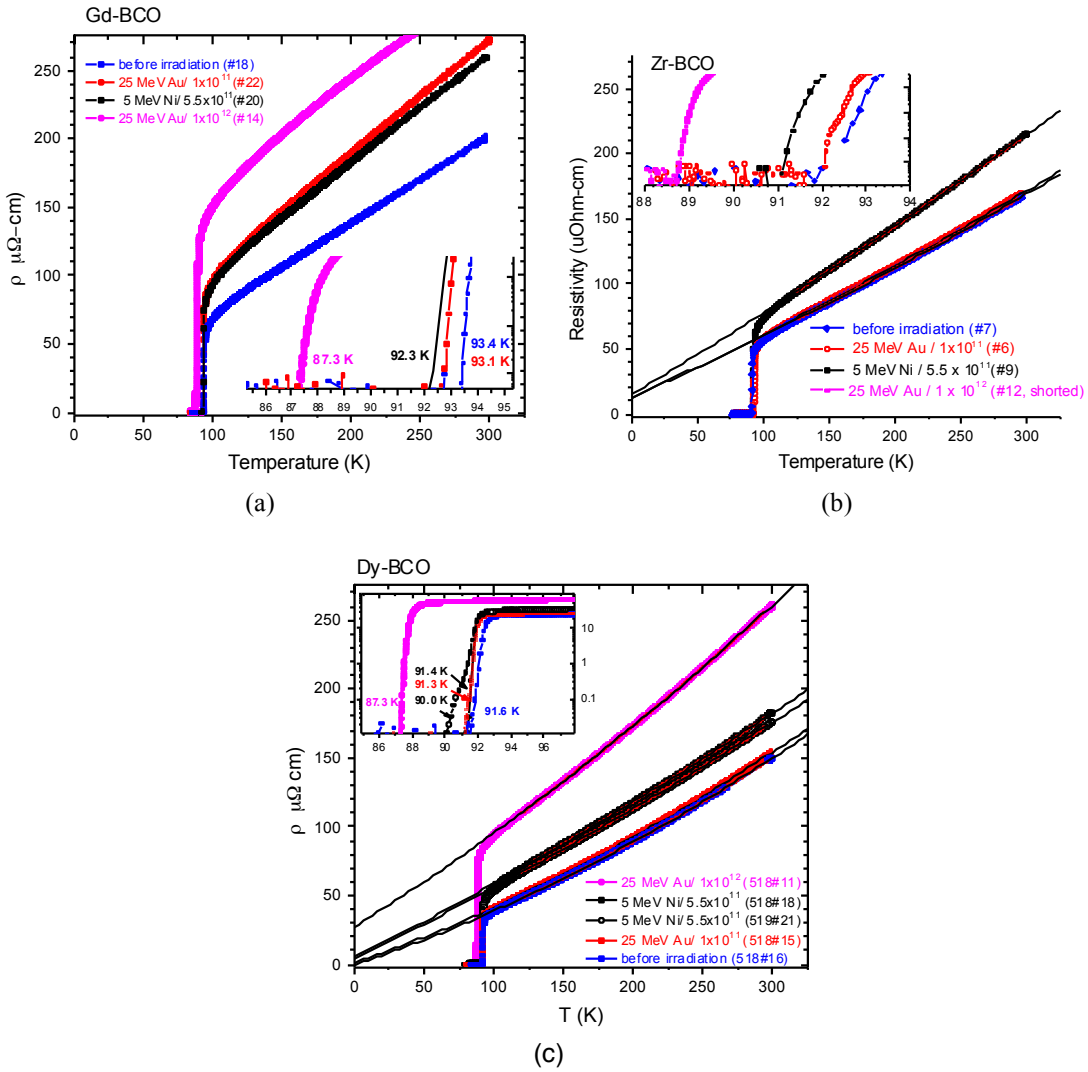

Figure 1. Transport resistivity versus temperature as a function of irradiation for the (a) $Gd_2Ba_2Cu_3O_{7-x}$, (b) Zr-doped $(Y,Gd)Ba_2Cu_3O_{7-x}$, and (c) $(Dy,Y)Ba_2Cu_3O_{7-x}$ conductors. Insert plots for each conductor show the change in critical temperature with irradiation.

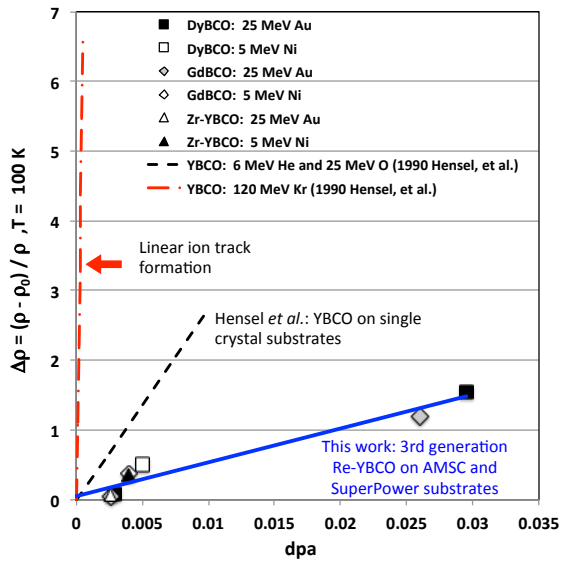

Figure 2. Change in 100 K resistivity from initial values (r_o) following ion irradiation of different superconducting films based on the YBCO conductor [1].

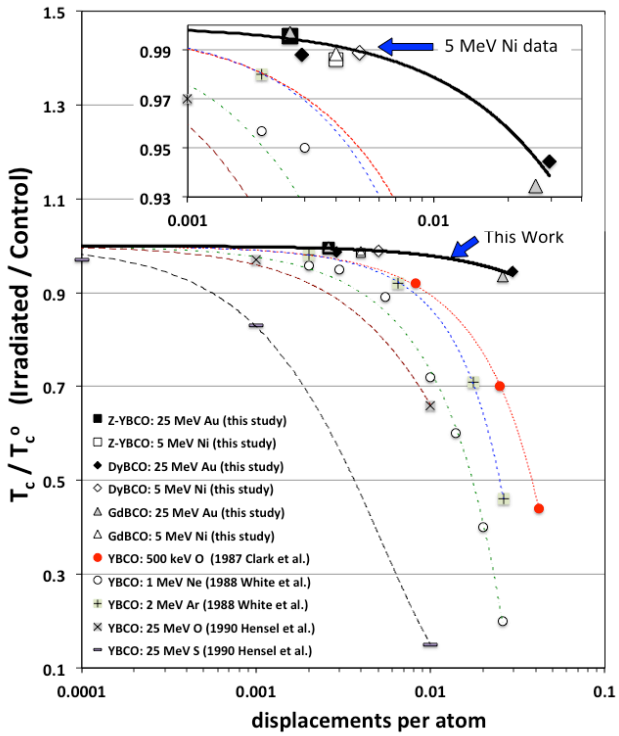

Figure 3. Change in T_c from initial values (T_c^o) as a function of displacement dose for ion irradiated conductors of this study compared to ion irradiation data of YBCO films deposited on single crystal substrates [1,3,4].

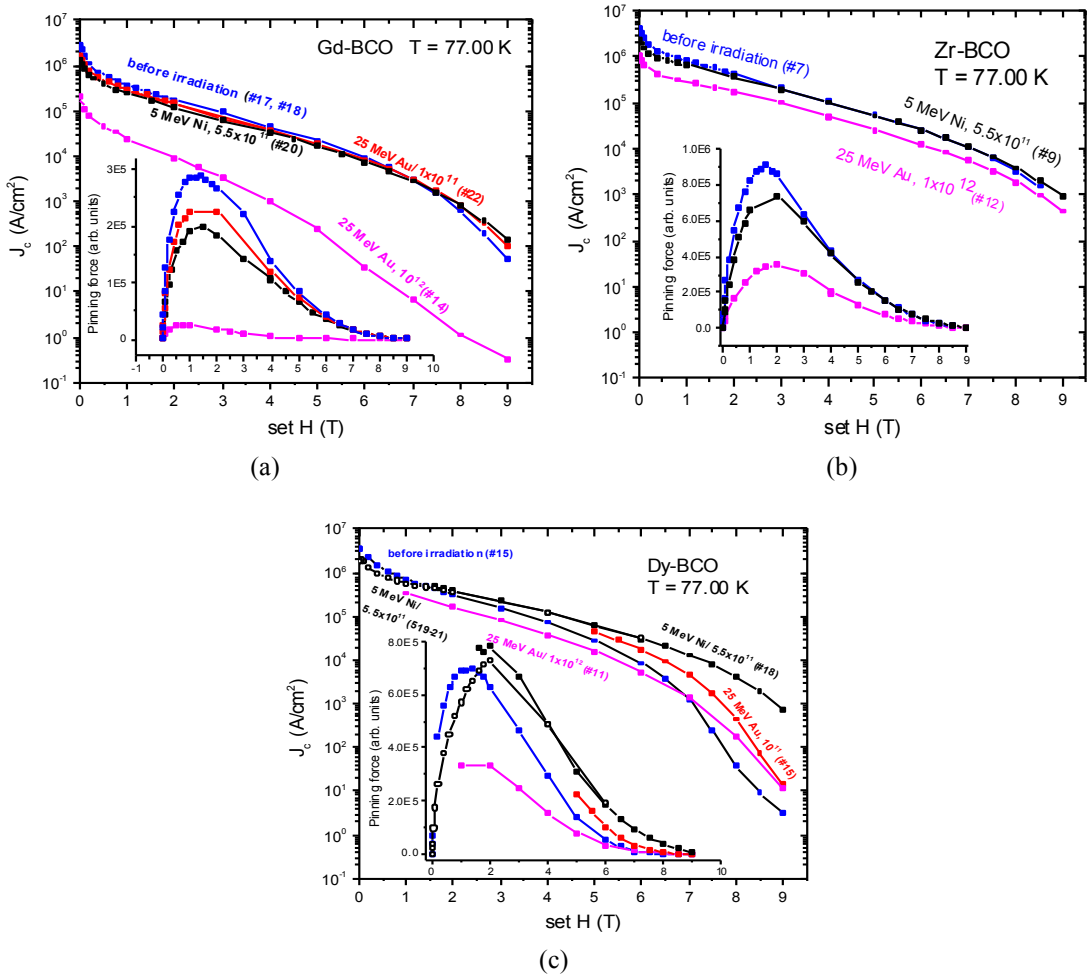

Figure 4. Transport critical current density (J_c) and pinning force (F_p) as a function of applied magnetic field strength for the (a) $Gd_2Ba_2Cu_3O_{7-x}$, (b) Zr-doped $(Y,Gd)Ba_2Cu_3O_{7-x}$, and (c) $(Dy,Y)Ba_2Cu_3O_{7-x}$ conductors following ion irradiation.

Ion irradiation of the Zr-YBCO conductor results in very little change in J_c even for the 0.03 dpa condition. Losses are measured in F_p with irradiation, which was shown by microscopy to be due to the reduction in $BaZrO_3$ (BZO) nanoparticles that are aligned in the c-axis direction within the conductor. However, this is offset by improved pinning in the *ab* direction by the increased amount of intergrowths generated at the interface with the BZO nanoparticles. This effect is not reflected in the results shown in Figure 4, as this data is collected in the H//c condition.

The DyBCO conductors showed a modest drop in transport properties for $H < 2$ T, but show a very pronounced improvement at the highest field strengths. This is also reflected in the increased F_p values particularly at $H > 3$ T. With the exception of GdBCO at 0.03 dpa, the J_c field dependence for the conductors is relatively unchanged for all test conditions for field strengths up to 6 T, above which J_c increases over the unirradiated values, and can be explained by the additional radiation induced defects in the microstructure [7,8]. The larger particles (Dy_2O_3 for example) in the conductors are effective pinning centers at higher

temperatures and lower field strength [7], but at higher fields (above 6T) the additional radiation-induced defects accommodate more flux pinning resulting in enhanced transport properties. The transport measurements suggest that improved irradiation stability of the conductors in this work is obtained through the presence of nanoparticles and associated correlated defects. These defects and interfaces can either act as sinks for displacement damage or initiate the creation of additional defect structures that can in turn provide different field orientation dependencies [8]. For example, the lack of irradiation-induced change of J_c performance for the Zr-doped YBCO films along H//c is a result of columnar BZO particles absorbing irradiation-induced damage in this direction while introducing new intergrowths that improve pinning along *ab*-planes. However, an opposite behavior is observed for the DyBCO conductors and is currently under investigation.

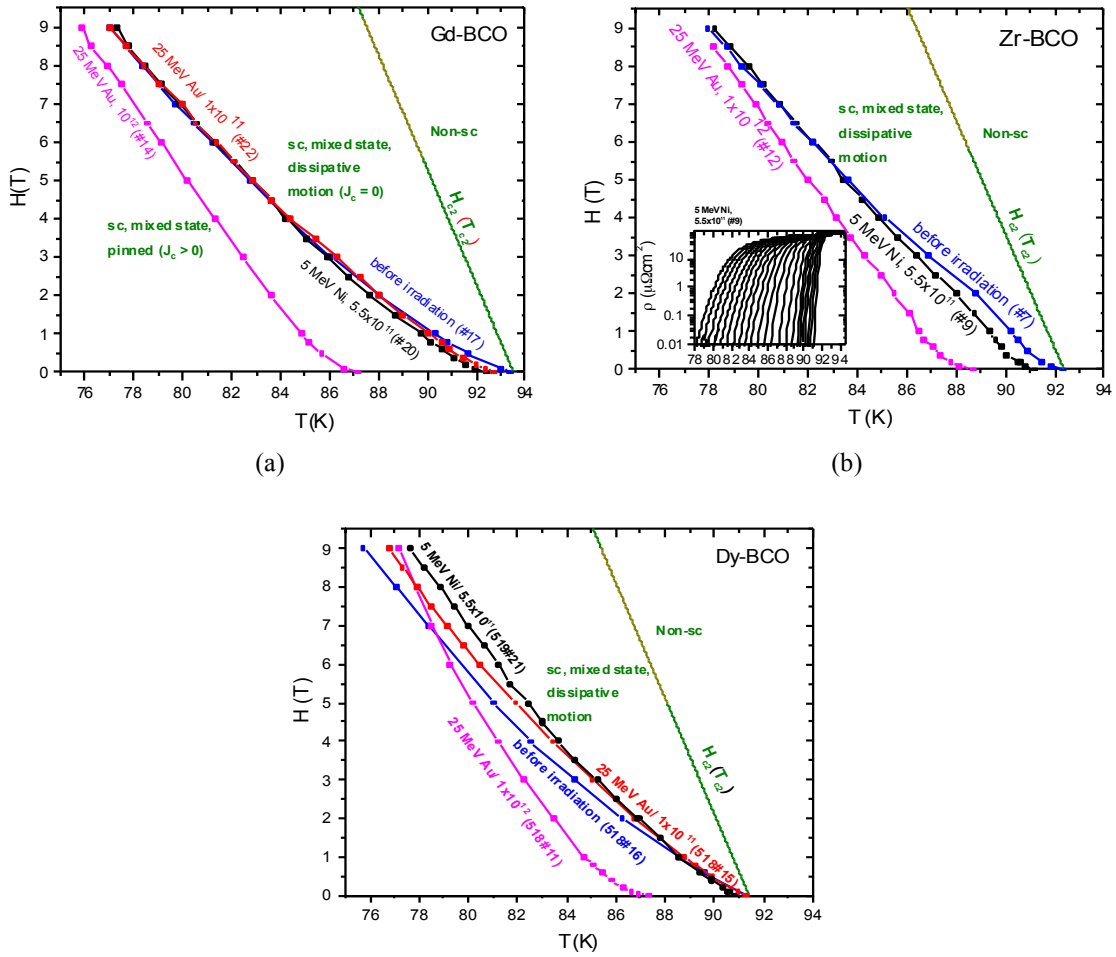

Figure 5. The irreversibility field as a function of temperature for (a) $Gd_2Ba_2Cu_3O_{7-x}$, (b) Zr-doped $(Y,Gd)Ba_2Cu_3O_{7-x}$, and (c) $(Dy,Y)Ba_2Cu_3O_{7-x}$ conductors following ion irradiation. The boundary of the upper critical field, $H_{C2}(T)$, is shown for each. The irreversibility field is the boundary where critical current falls below detectable levels, whereas the $H_{C2}(T)$ is the limit where bulk superconductivity is destroyed.

The use of YBCO conductors in large magnetic fields is limited by the characteristic irreversibility field, $H^*(T)$, which is lower than the upper critical field H_{c2}, and for which the values of J_c fall below detectible levels [9]. The irreversibility field, based on the effective pinning of flux-quantized line vortices by material imperfections such as point defects, grain boundaries, and secondary phases, is strongly dependent on the operating temperature and can vary from 27 Tesla at 52 K down to 5 Tesla at 80 K [9.10], where the benefit of a lower cost cryogenic cooling can be diminished by the field restrictions. The irreversibility line can be thought of as the depinning line or the boundary between pinned vortices and unpinned vortices. The changes in $H^*(T)$ for the conductors of this study following irradiation are shown in Figure 5, and show that following irradiation to 0.005 dpa no significant decrease to the usable phase space occurs. Much of the temperature reductions for a given field strength (or the available phase space lost) occur at lower field values for the high dose irradiations with the greatest reduction observed in the GdBCO conductor and least in the Zr-YBCO material. These temperature restrictions are minimized at the higher field strengths, particularly for the DyBCO conductor that shows improvements over the unirradiated value. It is likely that a similar effect is also observed in the other conductors for field strengths in excess of 9 T due to the observed presence of small (< 2 nm) radiation-induced defects appearing in the microstructures of all the conductors following 25 MeV Au irradiation to 0.03 dpa.

From the electrical characterization performed on the samples, the vortex creep rate (S) was determined as a function of the applied field strength. From combining the power law relationship between voltage and current with that of the Maxwell equation the creep rate is determined as $S = -\partial lnI/\partial lnt$. The lower the value of S correlates to minimizing the dissipative motion of the vortices, in which lower values are desirable to allow persistent-mode operation at the lowest voltages possible, without significant reduction in J_c. Following 5 MeV Ni irradiation the value of S shows a small increase in the GdBCO conductor, Figure 6, which converge slightly at higher fields with that of the unirradiated values. For the Zr-YBCO conductor there is little effect with irradiation to 0.004 dpa and a rise, though modest, with irradiation to 0.03 dpa. The DyBCO conductor is much more complex, in that a drop in S occurs for 0.003 – 0.004 dpa at applied fields above 2 T, and that the non-irradiated value increases to match the 0.03 dpa irradiation at higher fields. This confirms the pinning loss of the larger Dy_2O_3 particles (26 nm average size) at higher fields; where smaller radiation induced defects are more efficient. The relative lack of change in the Zr-YBCO conductor is not unanticipated as the material shows a measure of resilience to irradiation damage, though some shifting in the angular field dependent properties are observed. The loss in the small (3.8 nm average size) Gd_2O_3 particles with irradiation is very detrimental in the GdBCO, though radiation-induced defects may recover some properties in field strengths above 9 T.

CONCLUSIONS

The work conducted in the past year on the three commercial high temperature superconductors has shown generally promising results in terms of radiation tolerance. The behavior of each conductor type is different and shows improved radiation tolerance over earlier generation YBCO films. For the conditions investigated, the Zr-YBCO conductor shows the least amount of degradation with irradiation, with minor and localized changes in the microstructure related to the size and defects generated from the $BaZrO_3$ nanoparticles present within the conductor. The DyBCO conductor shows improved properties with irradiation damage to varying levels dependent on the applied magnetic field under which properties are tested. Though the GdBCO did not show as much tolerance to irradiation damage as the other conductor types, it is significantly improved over earlier generation YBCO base films.

CURRENT AND FUTURE WORK

Work currently being engaged involves the preparation of samples and irradiation holders for the neutron irradiation of the Zr-YBCO and DyBCO conductors. This work will take place at the High Flux Isotope Reactor within the 2014 calendar year. Further work involving transmission electron microscopy characterization of the ion-irradiated samples will be performed in order to elucidate specific phenomenon identified during electrical property evaluations. This includes identification of the causes for increased c-axis pinning in the DyBCO conductor at lower ion fluences as well as the nature of the faults generated and observed in the conductors at 0.03 dpa.

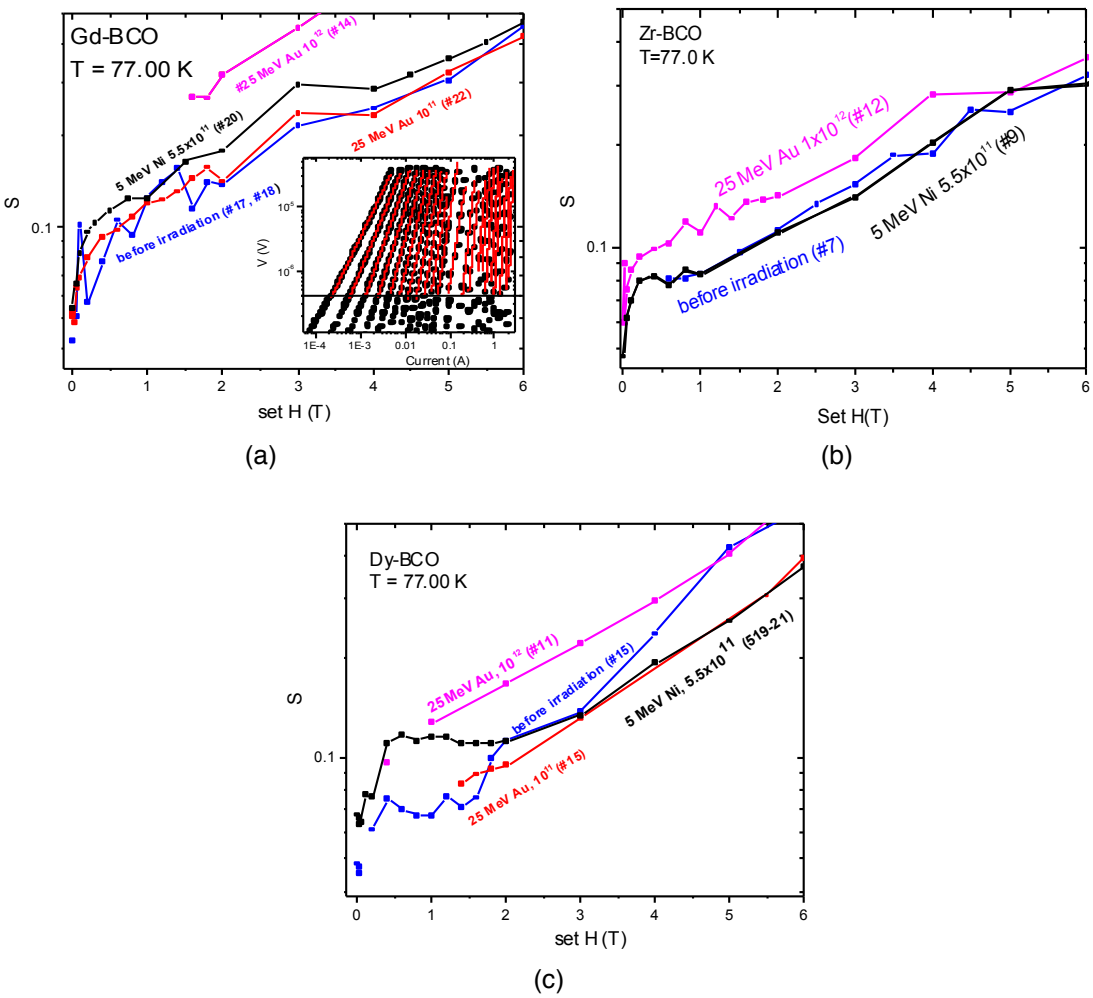

Figure 6. The vortex creep rate, *S*, as a function of applied magnetic field strength for (a) $Gd_2Ba_2Cu_3O_{7-x}$, (b) Zr-doped $(Y,Gd)Ba_2Cu_3O_{7-x}$, and (c) $(Dy,Y)Ba_2Cu_3O_{7-x}$ conductors following ion irradiation. The insert in (a) of voltage versus current is from the data taken in determining the value of *S*, with the steeper slope the better.

REFERENCES

1. B. Hensel et al., "Ion Irradiation of Epitaxial $YBa_2Cu_3O_{7-x}$ Films: Effects of Electronic Energy Loss," *Phys. Rev. B* **42** (7), 4135 (1990).
2. D. V. Kulikov et al., "Changes in the Transition Temperature After Irradiation and Annealing in Single Crystalline $YBa_2Cu_3O_{7-x,}$" *Physica C* **355**, 245 (2001).
3. G. J. Clark et al., "Effects of Radiation Damage in Ion Implanted Thin Films of Metal Oxide Superconductors," *Appl. Phys. Lett.* **51**, 139 (1987).
4. A. E. White, et al., "Ion-Beam Induced Destruction of Superconducting Phase Coherency in $YBa_2Cu_3O_{7-d}$," *Phys. Rev. B* **37** (7), 3755 (1988).
5. M. Okada and T. Kawakubo, "Effects of Neutron Irradiation on Superconducting Properties of Orthorhombic Y-Ba-Cu Oxides," *Rad. Eff. Defects Solids* **108**, 137 (1989).
6. M. Sawan, "Radiation Shielding Requirements for Magnets in Fusion Reactors," JAPMED-4 presentation, Cairo, Egypt, September 17-20, 2005.
7. U. Topal, L. Dorosinskii and H. Sozeri, "Effect of Neutron Irradiation on Pinning in SmBaCuO and YBaCuO Superconductors," *Physica C* **407**, 49 (2004).
8. M. Chudy et al., "Characterization of Commercial YBCO Coated Conductors After Neutron Irradiation," *IEEE Trans. Appl. Supercond.* **21** (3), 3162 (2011).
9. D. Larbalestier et al., "High T_c Superconducting Materials for Electric Power Applications," *Nature* **414,** 368 (2001).
10. R. M. Scanlan, A. P. Malozemoff, and D. C. Larbalestier, "Superconducting Materials for Large Scale Applications," *Proc. of the IEEE* **92** (10), 1639 (2004).